Synoptic weather patterns associated with intense ENSO rainfall in the southwest United States

N. Feldl[1] and G. H. Roe[2]

Received 10 September 2010; revised 28 October 2010; accepted 4 November 2010; published 14 December 2010.

[1] La Niña winters exhibit significant local enhancement of heavy rainfall in the southwest United States, relative to El Niño. This contrasts with average daily rainfall intensity, which is instead increased during El Niño winters. The present study explores the relationship between heavy rainfall and associated atmospheric circulation patterns. Using composite analysis, we find that heavy rainfall events in the southwest arise from the presence of a persistent offshore trough and simultaneous emplacement of a strong source of subtropical water vapor. Greater intensity of these storms during La Niña is consistent with a deeper offshore trough leading to strengthened moisture fluxes. Composite circulation patterns survive amongst a large degree of synoptic variability, highlighting the importance of understanding this variability when making regional climate predictions. **Citation:** Feldl, N., and G. H. Roe (2010), Synoptic weather patterns associated with intense ENSO rainfall in the southwest United States, *Geophys. Res. Lett.*, *37*, L23803, doi:10.1029/2010GL045439.

1. Introduction

[2] Understanding controls on heavy rainfall is a principle goal of climate impacts research, and for assessing natural hazard risk. One particular challenge centers on how such rainfall events respond to variability in large-scale atmospheric circulation. Characterizing storm climatology requires that a wide range of time and space scales must be tackled. The frequency, intensity, and spatial extent of rainfall all vary, and large-scale circulation depends on distant forcing. For instance, changes in tropical Pacific Ocean heating and convection comprising El Niño Southern Oscillation (ENSO) are associated with far-reaching temperature and rainfall anomalies [e.g., *Ropelewski and Halpert*, 1987; *Trenberth and Caron*, 2000]. Linking climate variability and associated regional weather impacts is of great public interest in affected regions (such as the southwest United States in the case of ENSO), and is particularly relevant to societal issues such as flood and landslide mitigation and reservoir management.

[3] Using ENSO as a case study of changes in midlatitude atmospheric circulation patterns, we investigate the synoptic fields associated with intense wintertime rainfall. Storm selection is based on daily rainfall over the southwest (SW) United States defined by 30.5–40°N, 116–126.25°W. Consistent with conventional wisdom, mean daily rainfall intensity is enhanced in the SW and suppressed in the northwest (NW) during El Niño winters, and vice versa during La Niña. However, contrary to expectations, *extreme* SW rainfall is locally enhanced during La Niña, and this result is significant in the regional average [*Feldl and Roe*, 2010].

[4] Figure 1a shows statistical analysis of daily rainfall as a function of intensity over the SW. This region exhibits strikingly coherent spatial rainfall patterns in the mean ENSO response; in particular, the northern boundary coincides with the northern extent of increases in mean daily rainfall intensity during El Niño winters. We apply the *t* test to the aggregate rainfall (i.e., lumping all events together without prior averaging over space or time) to evaluate the regional mean rainfall exceeding a given daily threshold. In the NW, for all thresholds considered, heavy rainfall conforms to the expected picture of increases during La Niña relative to El Niño. However in the SW (Figure 1a), La Niña rainfall overtakes El Niño as the threshold is raised. For thresholds exceeding 18 mm/day, La Niña actually exhibits a statistically significant increase in mean daily rainfall intensity in the SW, relative to El Niño.

[5] Figure 1b shows that diffuse increases in heavy La Niña rainfall over El Niño are apparent across the SW, although to a lesser degree in southernmost California. Much of the spatial structure of rainfall differences is likely determined by the relationship between mean wind direction and mountain range orientation, with flow perpendicular to the range leading to lifting along the windward flank and orographic rainfall. We also emphasize this is an intensity rather than frequency signal, and El Niño winters do indeed experience more frequent heavy SW rainfall, for all thresholds [*Feldl and Roe*, 2010]. Reconciling changes in frequency and intensity requires that La Niña receive a larger proportion of its total rainy days from extreme rainfall, compared to El Niño.

2. Data and Methods

[6] We seek to understand prevailing synoptic conditions during locally heavy wintertime (November through March) El Niño and La Niña rainfall. Three datasets are used:

[7] 1. Rainfall is obtained from CPC Unified Rain Gauge Database of gridded (0.25° × 0.25°) daily station data for 1948–1998 [*Higgins et al.*, 2000b]. Rainfall rates represent an average over each grid cell.

[8] 2. Strong ENSO events are selected based on the mean wintertime SST anomaly within the Niño 3.4 region (5°N–5°S, 170–120°W) [*Trenberth*, 1997] exceeding ±1 K (index available at http://www.cgd.ucar.edu/cas/catalog/climind/).

[1]Department of Atmospheric Sciences, University of Washington, Seattle, Washington, USA.
[2]Department of Earth and Space Sciences, University of Washington, Seattle, Washington, USA.

0094-8276/10/2010GL045439

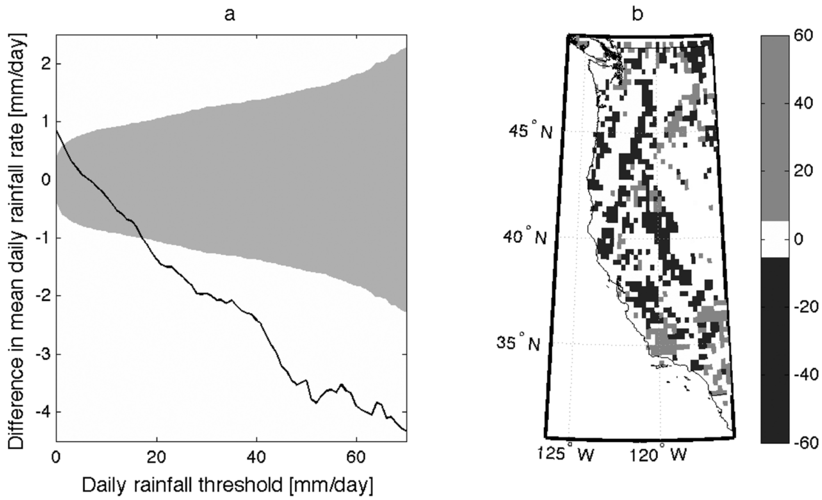

Figure 1. (a) Wintertime mean daily aggregate rainfall rate for El Niño minus La Niña as a function of threshold in the SW. Gray envelope indicates 95% confidence limits for the two-sample *t* test, after correcting for spatial and temporal correlation of rainfall data [*Bretherton et al.*, 1999; *von Storch and Zwiers*, 1999]. (b) Spatial patterns of percent differences in mean daily rainfall intensity (El Niño minus La Niña) for events ≥20 mm/day. Modified from *Feldl and Roe* [2010].

Our results are robust to varying definitions of ENSO [e.g., *Larkin and Harrison*, 2005].

[9] 3. Daily synoptic fields other than rainfall are from NCEP/NCAR Reanalysis [*Kalnay et al.*, 1996] for the same period as the rainfall.

[10] We index all La Niña and El Niño days which record heavy rainfall (defined as ≥20 mm/day) in the SW (for at least one grid cell). For La Niña, 384 days fit this criteria, or 34% of the total number of La Niña days in our 50-year window, and for El Niño, 526 days (43%). In the following section we present composites of synoptic state for heavy El Niño and La Niña rainfall in the SW. Figures 1–4 show unweighted composites, or in other words composites in which each day is weighted equally.

3. Results

3.1. Composite Analysis

[11] Figures 2a and 2b show mean daily 500 hPa geopotential height and relative vorticity for El Niño and La Niña storms. The relative vorticity reflects local flow curvature and highlights the position of the offshore trough. This mean circulation demonstrates characteristic ENSO features. Observed ridging of 500 hPa heights over the Rockies and associated split flow is typical of El Niño [*DeWeaver and Nigam*, 2002], and an eastward extension and poleward shift of the La Niña jet are apparent from the shift of the Pacific vorticity couplet (Figure 2b). Moreover, relative vorticity during La Niña storms (Figure 2b) is enhanced compared to El Niño (Figure 2a), suggestive of a deeper trough. SW rainfall is too distant to be attributed directly to large-scale vorticity advection. Rather other factors, such as frontal processes, must contribute.

[12] Figures 2c and 2d show composite 500 hPa geopotential height anomalies for heavy La Niña and El Niño rainfall. The daily anomalies are calculated by subtracting the smoothed (with a 30-day running mean filter) daily climatology from each day, hence highlighting the difference between our storm climatology and the evolving background state that occurs over the five-month winter. We see that for both El Niño and La Niña heavy SW rainfall is associated with a large offshore trough. These anomalies are statistically different from the mean field according to the *t* test at 5% significance (allowing for a 5% chance of identifying an anomaly where none exists). During La Niña the maximum anomaly is displaced northwards, but is deeper (17 m on average) and so also extends farther south. This deep offshore trough during La Niña storms in the SW is consistent with the enhanced vorticity field (Figure 2b).

[13] The 500 hPa trough is particularly persistent during heavy La Niña rainfall in the SW. We perform lagged composite analyses to evaluate persistence (not shown) and find that the trough survives for several days before and after heavy rainfall events. The e-folding timescale indicates the anomaly on average persists for 5 days after heavy rainfall. In comparison, the e-folding decay time of a 500 hPa anomaly (on all days) is only 3.4 days for a sample winter. Both decay times were calculated at the location of the composite trough maximum.

[14] Some insights into differences between El Niño and La Niña rainfall are apparent from composites of atmospheric moisture content and advection. Figure 3 shows column-integrated water vapor and 850 hPa wind for heavy rainy days (Figure 3, left) and all precipitating days (Figure 3, right) in the SW. Overall, heavy rainfall during both El Niño and La Niña is associated with enhanced offshore moisture, compared to all precipitating days. However the subtropical moisture reservoir is also slightly enhanced (in both area and magnitude) during heavy La Niña rainfall relative to El Niño. In addition, 500–1000 hPa geopotential thickness (not shown) indicates a warmer lower troposphere during La Niña storms and thus a higher moisture-carrying capacity.

[15] Figure 3 also shows the frequency distribution of wind direction for a SW coastal subregion (see wind rose insets). Focusing on heavy rainfall, on average we see more southwesterly winds during El Niño, consistent with general ENSO conditions (256° compared to 276° during La Niña), and strengthened moisture fluxes during La Niña relative to

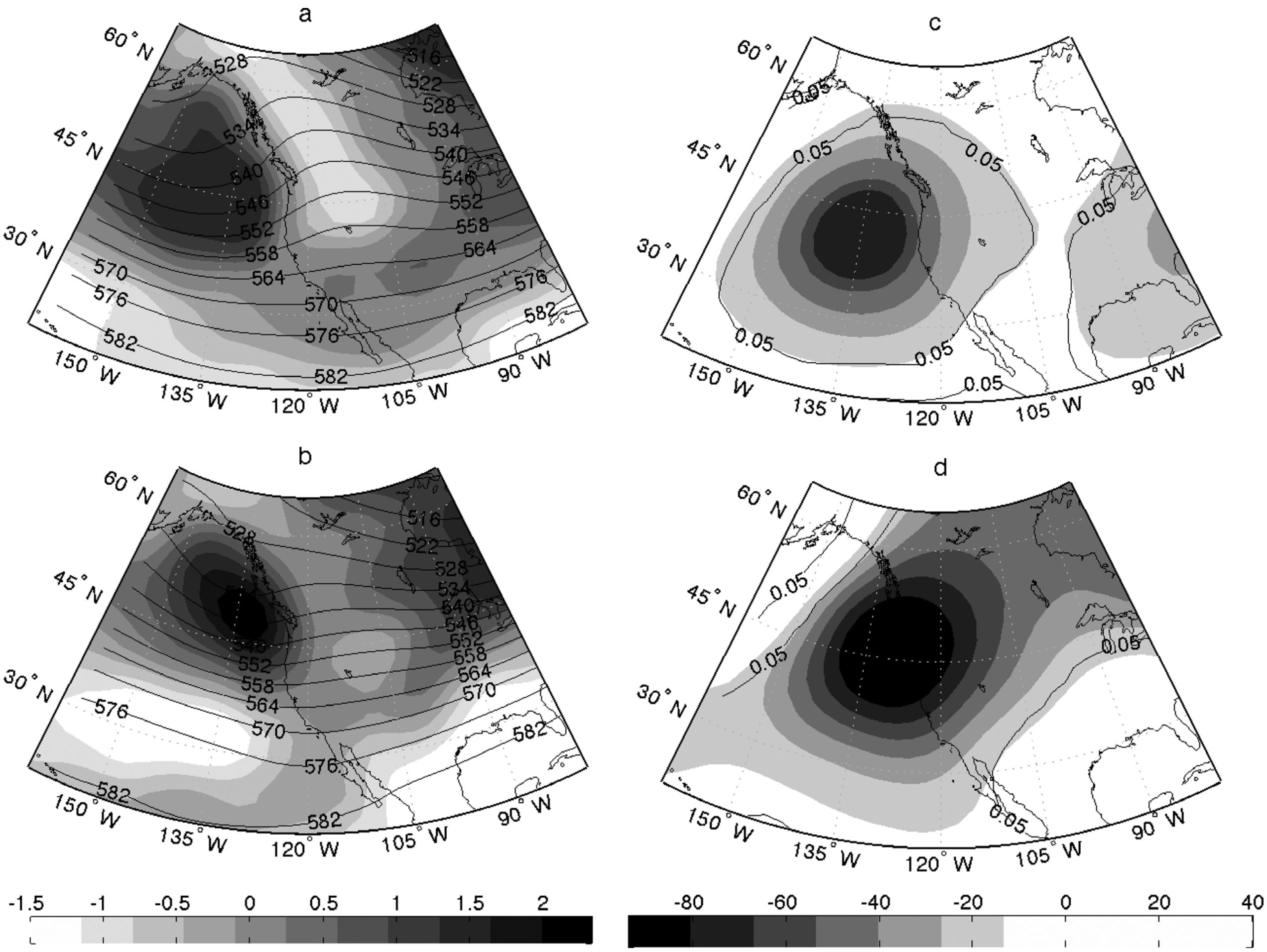

Figure 2. (left) Composite 500 hPa relative vorticity [10^{-5} s^{-1}] (shaded) and mean geopotential height [dam] (contours) for heavy SW rainfall. (top) El Niño and (bottom) La Niña. (right) Composite 500 hPa geopotential height anomalies [m], also for heavy SW rainfall. 95% confidence limits according to the *t* test are indicated by the solid contour. Heavy rainfall is defined as ≥20 mm/day.

El Niño (127 kg$(ms)^{-1}$ compared to 115 kg$(ms)^{-1}$, not shown). In both cases the moisture fluxes are larger than the climatological average or the ENSO average when the full range of rainfall is retained. Applying statistics (*t* test at the 5% significance level) to the aggregate data over this boxed subregion indicates that, while increases La Nina moisture content are not significant, changes in moisture flux and wind direction are.

[16] From Figure 3 the role of orographic enhancement on local rainfall patterns becomes apparent. Regions associated with flow impinging on the windward flank of mountain ranges during La Niña (e.g., Sierra Nevada) show increased heavy La Niña rainfall (cf. Figure 1b). Whereas mountain ranges instead oriented perpendicular to the more southwesterly El Niño winds (e.g., Transverse Ranges of Southern California) demonstrate increased heavy El Niño rainfall. Thus a combination of large-scale weather patterns and local effects determines the ENSO rainfall response.

[17] In summary of the compositing, heavy SW rainfall arises from the presence of a persistent offshore trough and simultaneous emplacement of a strong source of subtropical water vapor. Greater intensity of these storms during La Niña is consistent with a deeper offshore trough leading to significantly enhanced (and more westerly) moisture flux. This mechanism is comparable to the one proposed by *Higgins et al.* [2000a] to explain extreme rainfall events in the western U.S. However overall similarities in moisture content for Figures 3a and 3c suggest mean flow differences may in fact be of greater importance than moisture differences for heavy rainfall.

3.2. Variability

[18] Observed superposition of moisture and circulation anomalies shows some similarity to Pineapple Express events, a synoptic description of intensely-precipitating storms that impinge on the West Coast and originate as warm and wet air masses transported from the tropics near Hawaii [*Dettinger*, 2004]. However the well-defined, narrow plume of moisture that characterizes an atmospheric river is absent from our composite. Are atmospheric rivers simply washed out in the average? The record-breaking 1955 Christmas Eve storm that led to flooding in Yuba City, California [*Cole and Scanlon*, 1955] was concurrent with an offshore plume of tropically-sourced water vapor with column-integrated moisture values exceeding 40 kg m^{-2}. December of 1955 remains ranked as the wettest month on

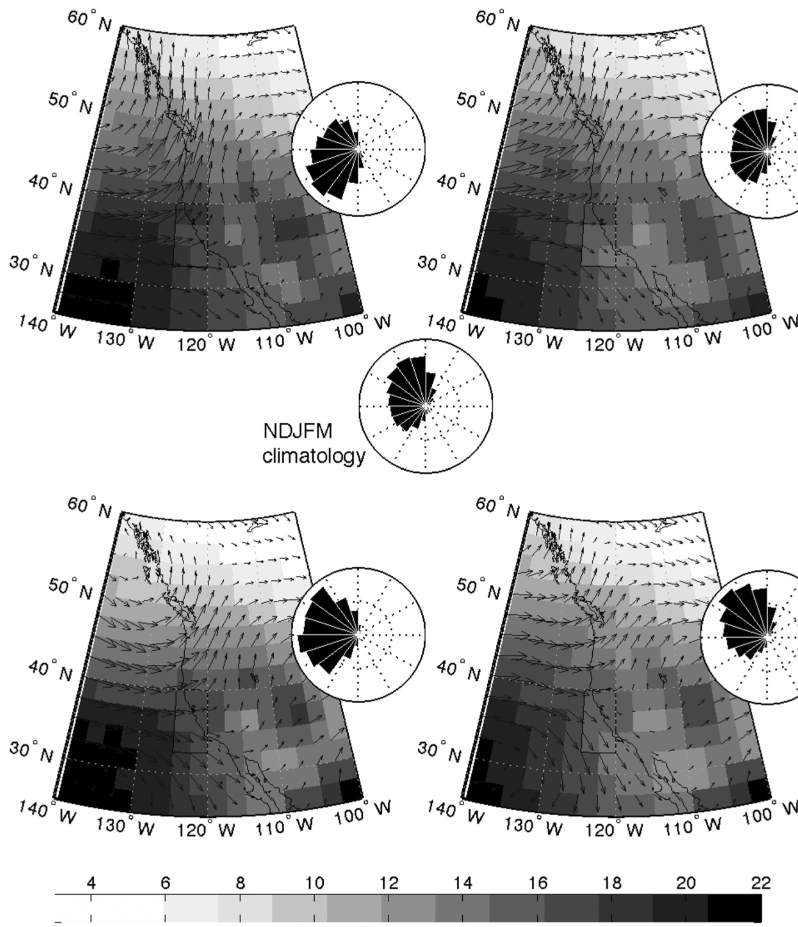

Figure 3. Composite column-integrated moisture [kg m^{-2}] (shaded) and 850 hPa winds (vectors) for (left) heavy SW rainfall (≥20 mm/day) and (right) all SW precipitating days. (top) El Niño and (bottom) La Niña. Inset plots show wind roses for the boxed subregion. The center rose plot indicates winter climatological values.

record for this region (according to the California Department of Water Resources northern Sierra Nevada eight-station index, available at http://www.cnrfc.noaa.gov/) with 30.83 inches of rainfall. This case is dramatic, but also leads one to wonder what fraction of daily composite members display distinctive Pineapple Express characteristics.

[19] We emphasize that composite members display a large degree of variability in circulation patterns. Figure 4 shows illustrative members of the La Niña storm composite, for column-integrated moisture and 500 hPa geopotential height. Deep troughs are prevalent (Figure 4a) and often lead to cut-off lows (Figure 4d) during La Niña storms in the SW. These patterns are reflected in composite 500 hPa geopotential height anomalies (Figure 2d). In contrast, during heavy El Niño rainfall, troughs tend to dig less deep, and we see more general southwesterly flow upstream of the SW (not shown).

[20] Focusing on column-integrated moisture, individual composite members exhibit a wide range of scenarios. The most common case is of moderate (~25 kg m^{-2}) moisture emplacement on the leading trough edge (Figure 4a). Only a fraction of heavy La Niña rainfall events (by visual inspection, no more than 20–25%) can be characterized as Pineapple Express-like storms (Figure 4c), whereas on other days the relationship between rainfall and synoptic conditions is more nuanced. Strong rainfall events also occur in the case of an offshore ridge (Figure 4b) and westerly flow (Figure 4e), and even during widespread lack of available moisture (Figure 4f). In considering the relationship between weather and climate, we note the large degree of variability exhibited in daily fields, and that the composite is a residual of this variability.

[21] Inspection of daily rainfall maps reveals that the largest La Niña storms tend to sweep across the entire western United States. This implicates trailing cold fronts in explaining heavy SW rainfall. Since cold fronts and associated rainfall tend to stretch along the trough axis, we expect concurrent (or leading by a day) heavy rainfall in the NW (as for ~88% of our heavy SW events). It is also the case that some La Niña storms do hit the SW coast only, with no associated heavy NW rainfall. And occasionally we see isolated grid cells of heavy rainfall, consistent with embedded frontal convective elements and perhaps concurrent with widespread drizzle.

4. Summary

[22] The goal of this analysis was to explore synoptic conditions behind an unusual and significant rainfall signal. We analyze atmospheric circulation patterns producing

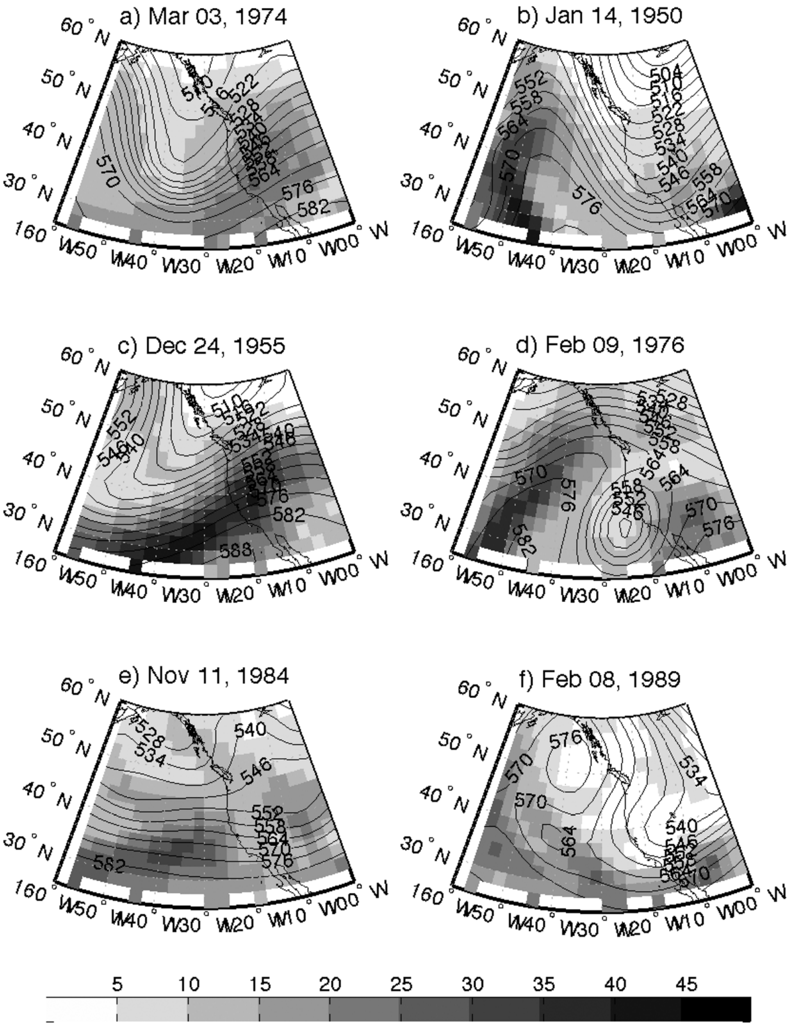

Figure 4. Composite members of column-integrated (1000–300 hPa) moisture [kg m^{-2}] (shaded) and 500 hPa geopotential heights [dam] (contours) for heavy (≥20 mm/day) La Niña rainfall in the SW.

enhancement of heavy La Niña rainfall in the southwest United States (even though the frequency of heavy rainfall is actually increased during El Niño). Big rain comes in big storms, and it should be emphasized that the ENSO variability discussed in this study reflects a small modification to this basic synoptic picture. Nonetheless, we establish important differences in rainfall intensity, circulation patterns, and moisture fields. In particular, composite analyses show that heavy La Niña rainfall is consistent with a persistent and deep offshore trough that taps into enhanced tropospheric moisture and advects it to the SW. Moisture flux into the SW is significantly larger during La Niña storms, and direction is significantly different.

[23] We emphasize the large amount of interstorm variability, with only a fraction of events fitting canonical Pineapple Express conditions. This behavior highlights the importance of understanding natural variability when making predictions of important atmospheric phenomena such as extreme rainfall. Depending on the impact of interest, be it frequency and spatial extent of heavy rainfall, or intensity of local rainfall, either El Niño or La Niña conditions may have the strongest effect.

[24] **Acknowledgments.** We thank Lynn McMurdie, Chris Bretherton, and Greg Hakim for insightful conversations. We are also grateful to three anonymous reviewers for thorough and constructive comments. This work was supported by the National Science Foundation (EAR-0642835).

References

Bretherton, C. S., M. Widmann, V. P. Dymnikov, J. M. Wallace, and I. Bladé (1999), The effective number of spatial degrees of freedom of a time-varying field, *J. Clim.*, *12*, 1990–2009.

Cole, R. O., and J. P. Scanlon (1955), Flood-producing rains in northern and central California, December 16–26, 1955, *Mon. Weather Rev., December 1955*, 336–347.

Dettinger, M. (2004), Fifty-two years of “Pineapple-Express” storms across the West Coast of North America, *PIER Proj. Rep. CEC-5000-2005-004*, U.S. Geol. Surv., Scripps Inst. of Oceanogr. for the Calif. Energy Comm., La Jolla.

DeWeaver, E., and S. Nigam (2002), Linearity in ENSO’s atmospheric response, *J. Clim.*, *15*, 2446–2461.

Feldl, N., and G. H. Roe (2010), Climate variability and the shape of daily precipitation: A case study of ENSO and the American West, *J. Clim.*, doi:10.1175/2010JCLI3555.1, in press.

Higgins, R. W., J.-K. E. Schemm, W. Shi, and A. Leetmaa (2000a), Extreme precipitation events in the western United States related to tropical forcing, *J. Clim.*, *13*, 793–82.

Higgins, R. W., W. Shi, E. Yarosh, and R. Joyce (2000b), Improved United States precipitation quality control system and analysis, *NCEP/Clim. Predict. Cent. ATLAS 7*, NOAA, Silver Spring, Md.

Kalnay, E., et al. (1996), The NCEP/NCAR reanalysis 40-year project, *Bull. Am. Meteorol. Soc.*, *77*, 437–472.

Larkin, N. K., and D. E. Harrison (2005), On the definition of El Niño and associated seasonal average U.S. weather anomalies, *Geophys. Res. Lett.*, *32*, L13705, doi:10.1029/2005GL022738.

Ropelewski, C. F., and M. S. Halpert (1987), Global and regional scale precipitation patterns associated with the El Niño/Southern Oscillation, *Mon. Weather Rev.*, *115*, 1606–1626.

Trenberth, K. E. (1997), The definition of El Niño, *Bull. Am. Meteorol. Soc.*, *78*, 2771–2777.

Trenberth, K. E., and J. M. Caron (2000), The Southern Oscillation revisited: Sea level pressures, surface temperatures, and precipitation, *J. Clim.*, *13*, 4358–4365.

von Storch, H., and F. W. Zwiers (1999), *Statistical Analysis in Climate Research*, 484 pp., Cambridge Univ. Press, Cambridge, U. K.

N. Feldl, Department of Atmospheric Sciences, University of Washington, 408 ATG Bldg., Seattle, WA 98195-1640, USA. (feldl@u.washington.edu)

G. H. Roe, Department of Earth and Space Sciences, University of Washington, 070 Johnson Hall, Seattle, WA 98195-1310, USA.